03,05

# Creation of GaMnAs ferromagnetic semiconductor by combined laser method

© O.V. Vikhrova[1], Yu.A. Danilov[1], D.A. Zdoroveyshchev[1], I.L. Kalentyeva[1], A.V. Kudrin[1], V.P. Lesnikov[1], A.V. Nezhdanov[1], A.E. Parafin[2]

[1] Lobachevsky State University,
Nizhny Novgorod, Russia
[2] Institute for Physics of Microstructures, Russian Academy of Sciences,
Nizhny Novgorod, Russia
E-mail: vikhrova@nifti.unn.ru

*Received March 24, 2023*
*Revised March 24, 2023*
*Accepted March 28, 2023*

GaMnAs layers made by pulsed laser deposition in vacuum on semi-insulating GaAs substrates have been studied. During the creation of the structures, the substrate temperature varied in the range from 200 to 350°C, and the thickness of the layers was $\sim 50$ nm. Samples of the manufactured structures were annealed by pulses of an excimer KrF-laser. The analysis of the Raman scattering spectra of annealed samples using their approximation by Lorentz functions showed, in addition to peaks in the LO- and TO-GaAs modes, the presence of a coupled phonon-plasmon mode. As a result of annealing, a significant increase in the hole conductivity of the layers is observed (the resistance decreases from $R_s \sim 10^7-10^9\,\Omega$ to $R_s \sim 900-3000\,\Omega$). The type of magnetic field dependence of magnetization at room temperature changes significantly: there is a transition from a nonlinear characteristic with a hysteresis loop for the initial sample (appearing due to the presence of MnAs compound inclusions with a Curie temperature above room temperature) to a linear behavior for the annealed sample. The study of galvanomagnetic properties at temperatures from 10 to 150 K shows the existence of ferromagnetism in GaMnAs layers with a Curie temperature reaching 90 K. The observed effects allow us to conclude that the applied pulsed laser action leads to modification (dissolution) of MnAs inclusions, electrical activation of Mn and, as a consequence, to the formation of a single-phase ferromagnetic semiconductor GaMnAs.

**Keywords:**: pulsed laser deposition, pulsed laser annealing, ferromagnetic semiconductor.

DOI: 10.21883/PSS.2023.05.56042.43

## 1. Introduction

Relevance of ferromagnetic semiconductor (FMS) physics and technology studies is constantly growing. Focus is made on their application primarily in logical and nonvolatile memory devices [1]. A recently adopted change in the magnetic semiconductor terminology shall be noted herein. They are subdivided into diluted magnetic semiconductors (DMS), including primarily $A^{II}B^{VI}$ type heavily manganese-doped semiconductors, and ferromagnetic semiconductors (FMS), including $A^{III}B^{V}$ manganese- or iron-doped semiconductor compounds, elemental semiconductors (Ge : Mn, Ge : Fe) and some other materials (in particular, wide-band oxides doped with transition atoms) that exhibit ferromagnetic properties besides semiconductor properties. A new persistent trend in the international spintronics literature includes the study and application of these materials in $A^{III}B^{V}$ heavily iron-doped semiconductor device structures. Initially (since 2012), these were InFeAs and GaFeSb narrow-band semiconductors, then the list of these compounds has been extended. According to the recent review of spin electronics publications [1–5], ferromagnetic semiconductors have a great future, because they enable, in particular, magnetic property control by an electric field (as opposed to metals where such control is not possible) [2], creation of spin vertical field-effect transistors [1], resonance tunnel diodes [6], spin-orbit torque magnetization switching devices [2] (with required spin-polarized current densities 2−3 orders of magnitude lower than for ferromagnetic metals) and other devices (sensors, storage elements) with improved high speed response and low power consumption.

It should be noted that GaMnAs FMS is still addressed as the main prototype material used to optimize the concepts, topology and design of spintronics devices, despite the fact that its Curie temperature is lower than room temperature. Therefore, the investigations of methods for production of GaMnAs layers compatible with mass semiconductor production are very important. Low-temperature molecular-beam epitaxy (LT-MBE), it the main method for production of GaMnAs layers, because it ensures high manganese solubility in group III atom sublattice and, thus, allows to produce a material with high concentrations of charge carriers (holes). According to the existing theories describing ferromagnetism mechanism in GaMnAs layers, the Curie temperature and degree of spin polarization of charge carriers depend on the concentrations of magnetic impurity atoms and charge carriers [7]. For GaMnAs

semiconductor, the Curie temperatures of $\sim 170$ K were achieved with a manganese concentration of 3−5 at.% [8]. At the same time, an increase in the amount of manganese to be introducted during growth higher than 10 at.% in the GaMnAs system results in a decrease of its electrical activity and formation of second ferromagnetic phase MnAs inclusions [9]. Clusters in FMS are formed due to low equilibrium solubility threshold of transition elements (in particular Mn). Formation of the second phase as MnAs nanoinclusions during GaMnAs production is a priori considered as an undesired process, because it is believed to destroy the crystalline matrix structure and prevent the achievement of the desired high concentration of magnetic moments and charge carriers. In addition to the problem mentioned above, it should be noted that the LT-MBE capabilities of efficient crystalline quality, magnetic, optical and electrical properties control for the produced GaMnAs layer structures are exhausted to a great extent. It should be also noted that the issue of exerting any effect on ferromagnetic semimetallic clusters after they have been already formed in a semiconductor is virtually not investigated. Only [10] should be noted where continuous laser exposure at high temperature (up to 580°C) somehow modified the geometry (reduced the dimensions) of small-size (up to 12 nm in diameter) MnAs clusters in GaMnAs matrix, with the result depending to some extent on the laser emission wavelength. It should be noted that the phenomenon is attributed to the optical absorption with the involvement of quantum levels in MnAs clusters, and the effect was not evident enough to be recommended as a production technique.

A method of pulsed laser deposition in vacuum or gas atmosphere holds promise for use in production of $A^{III}B^{V}$ based materials. Combination of pulsed laser deposition and postgrowth laser annealing methods are of particular interest. Previously, we have published findings of a similar study of structures produced by pulsed laser deposition method at low pressure in gas atmosphere (hydrogen with addition of arsine) that feature a GaMnAs layer thickness from 150 to 400 nm and were subjected to postgrowth pulsed laser annealing [11]. New opportunities were demonstrated to find mechanisms and processes facilitating additional electrical activation of the injected impurity, the Curie temperature increase, defect concentration reduction in layers and second phase clusters exposure (MnAs).

The study of GaMnAs ferromagnetic semiconductor produced by a combination of low-temperature pulsed laser deposition in vacuum (PLD-V) and pulsed laser annealing (PLA) methods is described herein.

## 2. Experiment procedure

GaMnAs layers were deposited on $i$-GaAs (100) substrate (with deflection 2° towards [110]) by means of solid target (undoped GaAs and high-purity manganese) sputtering by focused YAG : Nd second harmonic laser (532 nm, pulse energy 280 mJ, pulse duration 10 ns, beam area on the target $\sim 1.5\,\text{mm}^2$). When producing GaMnAs/GaAs structures, the process temperature ($T_g$) was varied from 200 to 350°C. The content of manganese was assessed by the ratio of the amounts of laser-evaporated metal and semiconductor and was equal to $Y_{\text{Mn}} = 0.17$ (technological assessment), layer thickness achieved $\sim 50$ nm. The samples of the produced structures were subjected to pulsed lase annealing using LPX-200 eximer laser (KrF 248 nm, pulse duration 30 ns, laser fluence $P = 400\,\text{mJ/cm}^2$). Structural properties of initial and irradiated samples were studied by Raman scattering spectroscopy (RSS). RS spectra were measured at room temperature using NTEGRA Spectra system with 473 nm laser. Emission was focused by 100× NA = 0.9 lens. Laser output power measures using 11PD100-Si (Standa Ltd) silicon photodetector was equal to 0.5 mW. RS spectra were analyzed within 50−900 $\text{cm}^{-1}$ with resolution 0.7 $\text{cm}^{-1}$. The exposure time was 120 s.

Magnetization of the initial and annealed structures was measured at room temperature by a field alternating gradient magnetometer. Galvanomagnetic properties of structures were studied using Keithley 2400 source measurement unit and Janis CCS-300S/202 closed-loop helium cryostat at 10−300 K in magnetic field range ±3600 Oe. At room temperature, Hall effect measurements were carried out in a magnet field up to 2.8 T. This ensured proper measurement of the type of conductivity, normal Hall effect constant ($R_0$), charge carrier mobility and concentration in annealed samples.

## 3. Findings and discussion

All GaMnAs layers produced by the pulsed laser deposition method show high layer resistances ($R_s$) at room temperature (Table 1). It is shown that layer resistance $R_s$ increases from $\sim 10^7$ to $\sim 10^9\,\Omega$ with the increase in the GaMnAs layer formation temperature from 200 to 350°C. After pulsed laser annealing, the conductivity of GaMnAs films increase significantly ($R_s \sim 880{-}2970\,\Omega$). Hole concentration $p$ calculated using the Hall effect measurements achieves $\sim 2.8 \cdot 10^{20}\,\text{cm}^{-3}$ and effective mobility is $\mu_{\text{eff}} \sim 4{-}5\,\text{cm}^2/\text{V} \cdot \text{s}$. This fact is indicative of activation processes appearing under the influence of the pulsed laser annealing resulting in the incorporation of manganese atoms into the position of substitution of gallium atoms and, thus, providing the hole conductivity. It is apparent that at lower layer formation temperatures (200 and 250°C), the degree of electrical activation of the impurity is much higher (Table 1).

Raman scattering spectroscopy measurements of the initial and laser annealed GaMnAs/GaAs structures are shown in Figure 1, $a$. RS spectra of the produced structures contain an intense narrow peak near LO-mode (291 $\text{cm}^{-1}$) and a weakly pronounced peak for TO-mode (268 $\text{cm}^{-1}$) of crystalline GaAs in accordance with the sampling procedure for back scattering geometry. The

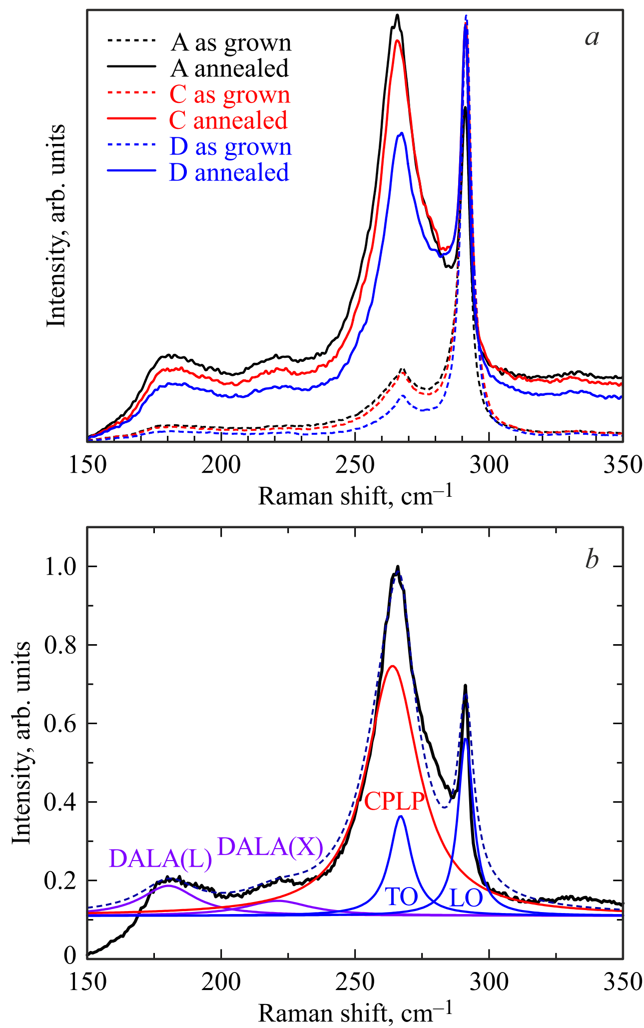


**Figure 1.** *a* — RS spectra of GaMnAs layers grown by the PLD method at various temperatures and subjected to pulsed laser annealing. *b* — Lorentzian approximation of the RS spectrum of GaMnAs layer grown at 250°C and laser annealed. LO- and TO modes of GaAs, coupled phonon-plasmon (CPLP) mode and disorder activated modes (DALA (L), DALA (X) as shown).

presence of TO-mode may be attributed to disordering in the GaMnAs layer due to heavy manganese doping and to some back scattering geometry abnormalities and (or) substrat orientation deflection from plane (100). After pulsed laser exposure, considerable decrease in the intensity of LO-mode is observed. Peak near TO-mode of GaAs is expanded, its intensity grows considerably, in particular for the samples produced at 200 and 250°C (cases of maximum hole concentrations after pulsed laser annealing). The RS spectra analysis of the annealed samples using Lorentzian approximation has shown (Figure 1, *b*) that, in addition to peaks near LO- and TO-modes of crystalline GaAs, the spectra contain a coupled phonon-plasmon mode (CPLP) [12,13]. The coupled phonon-plasmon mode is formed as a result of interaction between longitudinal optical phonons and plasmons, its intensity and position

**Table 1.** Electrical properties (at 300 K) of structures with GaMnAs layer produced by the pulsed laser deposition method (initial and pulsed excimer laser annealed).

| Structure | $T_g$, °C | Initial sample | Sample after PLA | | |
|---|---|---|---|---|---|
| | | $R_s$, Ω | $R_s$, Ω | $\mu_{\text{eff}}$, cm$^2$/V · s | $p$, cm$^{-3}$ |
| A | 200 | $7 \cdot 10^7$ | 920 | 5 | $2.6 \cdot 10^{20}$ |
| B | 250 | $1.3 \cdot 10^8$ | 880 | 5 | $2.8 \cdot 10^{20}$ |
| C | 300 | $7.6 \cdot 10^8$ | 1200 | 5 | $2.2 \cdot 10^{20}$ |
| D | 350 | $1.5 \cdot 10^9$ | 2970 | 4 | $1.2 \cdot 10^{20}$ |

**Table 2.** Position of the main phonon modes calculated by means of Lorentzian approximation of the RS spectra for laser annealed GaMnAs/GaAs structures

| $T_g$, °C | 200 | 250 | 300 | 350 |
|---|---|---|---|---|
| $\omega_{\text{TO}}$, cm$^{-1}$ | 267 | 267 | 267 | 267 |
| $\omega_{\text{LO}}$, cm$^{-1}$ | 291 | 291 | 291 | 291 |
| $\omega_{\text{CPLP}}$, cm$^{-1}$ | 265 | 264.8 | 266.5 | 270 |

in the spectrum depend on the plasmon density (hole concentration herein). Moreover, owing to crystal lattice disordering, peaks occur in the RS spectra which are caused by the activation of longitudinal acoustic phonon modes in X-points (DALA(X)) and L-points (DALA(L)) of Brillouin zone which are usually forbidden in the first-order Raman scattering spectrum [12,13].

Table 2 shows the Lorentz function approximations of the RS spectra for laser-annealed GaMnAs/GaAs structures grown at various temperatures: frequency positions of LO-, TO- and CPLP-modes.

It is widely known that interaction between LO-phonon and electronic plasmon for *n*-type GaAs at high electron concentration results in the appearance of two peaks in the Raman scattering spectrum $L_+$ and $L_-$. In the first case, a strong blue movement is observed when the electron concentration increases, in the second case — position of $L_-$ mode remains virtually stationary close to TO-phonon frequency. In *p*-type GaAs, due to strong hole plasmon attenuation, only one phonon-plasmon mode is observed which is moved from LO- to TO-frequency when the hole concentration increases. In other words, CPLP mode in *p*-GaAs spectrum is usually located between TO and LO modes (in the range from 268 to 291 cm$^{-1}$) [14]. At the same case, when the impurity concentration is high (for manganese it is 3 at.% and higher), phonon-plasmon mode below TO-mode (red frequency movement) is observed due to the strain taking into account the impurities [12,13]. Figure 2 shows position of the coupled phonon-plasmon mode at various hole concentrations which can be compared with data reported in [13] for GaMnAs layers with manganese content up to 8.3% produced by the low-temperature molecular-beam epitaxy method. Our Raman scattering

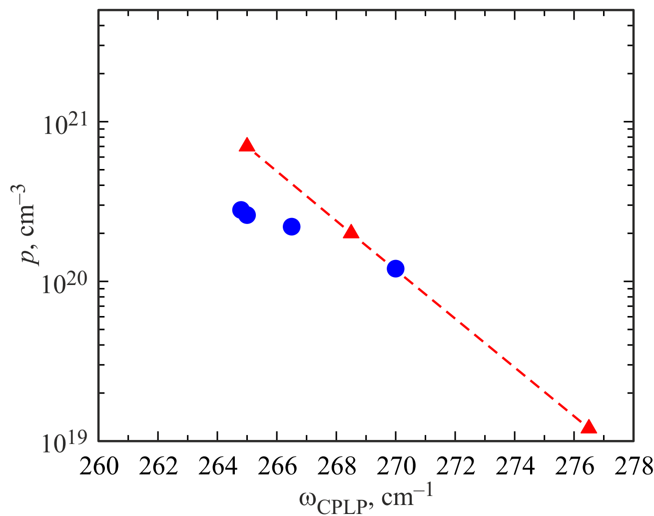


**Figure 2.** Hole concentration and frequency position of the coupled phonon-plasmon mode for laser annealed GaMnAs/GaAs structures. Data (dashed line and triangles) reported in [13] for GaMnAs with manganese content up to 8.3% produced by the LT-MBE method are also shown.

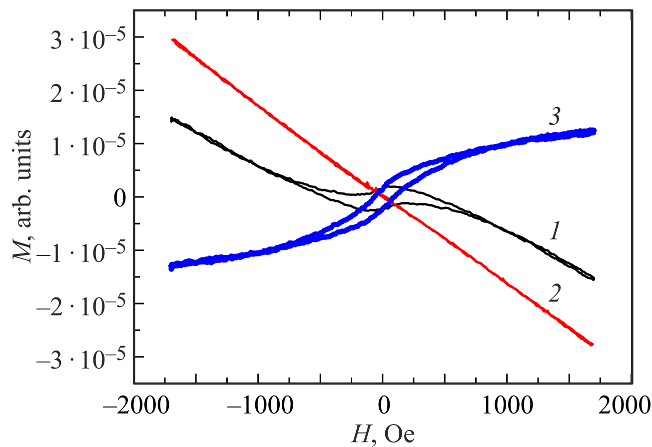


**Figure 3.** Magnetic field dependences of magnetization at room temperature for the initial (curve *1*) and annealed (curve *2*) structure sample with GaMnAs layer produced at 300°C. External magnetic field was applied in the layer plane. Dependence *3* (corresponding to $M(H)$ of GaMnAs layer) was obtained by subtraction of curve *2* (meeting the diamagnetic contruibuiion of the GaAs substrate) from curve *1*.

spectroscopy results obtained for GaMnAs/GaAs structures produced by the pulsed laser deposition in vacuum and laser annealed are in good agreement with this reported data.

Pulsed lase annealing has a significant impact on the magnetic properties of GaMnAs layers. In particular, after PLA, considerable change in the form of magnetic field dependence of magnetization ($M(H)$) at room temperature is observed. Thus, for all initial samples, nonlinear characteristics $M(H)$ with hysteresis loop were observed due to the presence of ferromagnetic MnAs inclusions with the Curie temperature above room temperature (Figure 3, curve *1*). In case of annealed samples, dependences $M(H)$ are linear and depend on the diamagnetic behavior of GaAs substrate (Figure 3, curve *2*). The magnetic field dependence of magnetization of the GaMnAs layer itself (curve *3* obtained by subtraction of curve *2* from curve *1*) contains hysteresis with coercive field about 80 Oe and does not achieves saturation in the range of the used magnetic fields. The latter may be due to the contribution of the paramagnetic component and/or magnetization vector orientations at an angle to the layer plane.

An attempt will be made below to interpret the obtained variation effects of the magnetic field dependences of magnetization for the laser annealed samples taking into account the previously represented analysis of property modification in heteronanostructures with GaMnAs layer on the surface due eximer laser exposure [15]. In the quoted publication, the GaMnAs layer on the surface of the quantum-size heterostructure was produced by the pulsed laser deposition at low pressure in carrier gas atmosphere (hydrogen with addition of arsine). For such structures, design temperature distributions in the sample as a result of PLA eximer laser absorption were obtained. The initial laser exposure simulation conditions were defined by the optical properties of the GaMnAs layer in the eximer laser wavelength (reflectance and absorbance, loss of emission due to scattering caused by rough surface), thermal conductivity coefficient and layer thickness [15]. Moreover, the obtained temperature dependences of the thermal conductivity coefficient ($k$) of the initial heteronanostructures with GaMnAs layer were used and it was found that, for the temperature range from 20 to 100°C, the thermal conductivity coefficient of GaMnAs was 1.5–2 as low as for GaAs (at 20°C $k$ was equal to 38.5 and 59 W/m · K for (Ga, Mn)As and GaAs, respectively) [11]. Calculations of the temperature distribution along the sample thickness and in time taking into account this data have shown that a temperature close to the GaAs melting temperature (1515 K) may be achieved in the subsurface thin GaMnAs layer (10–20 nm) due to laser emission absorption. Melting temperature of equiatomic MnAs is also known and is equal to 936°C (1209 K) [16]. Therefore, the laser exposure provides conditions when the temperature in the GaMnAs layer is much higher than the specified value and, thus, it may be expected that the MnAs inclusions with a lower melting temperature than that of the matrix may by modified substantially in the annealed sample. Modification may mean partial or total decomposition of MnAs inclusions, diffusion and integration of manganese atoms into the gallium atom substitution positions, as a result the hole concentration increase dramatically and considerable reduction of the layer resistance is recorded in the annealed samples. It also may be expected that the thinner the GaMnAs layer is, the higher the probability of such modification is. This conclusion is supported by the results reported by us earlier in [11] for GaMnAs/GaAs structures with manganese content $Y_{\text{Mn}} \sim 0.13{-}0.15$ (technological assessment) produced

by the pulsed laser deposition method in gas atmosphere at 330°C and exposed to eximer laser. In particular, it has been shown that considerable changes in the ferromagnetic MnAs inclusions occur for a structure with 150 nm GaMnAs layer. Due to these changes, no response from MnAs phase is recorded in the X-ray diffraction spectrum, clusters are not visible on the high resolution transmission electron microscopy image of the annealed sample and the magnetic field dependence of magnetization at room temperature shows the absence of ferromagnetization [11].

On the other hand, all temperature dependences of layer resistance of the annealed GaMnAs/GaAs structures contain maxima (shown by arrows) caused by the ferromagnetic–paramagnetic phase transition (Figure 4). The Figure shows the temperatures corresponding to these resistance maxima ($T_{max}$). This temperature is generally accepted as the Curie temperature. Magnetic field dependences of Hall resistance at temperatures lower than $T_{max}$ are nonlinear with a hysteresis loop and negative magnetoresistance is observed with regions corresponding to anisotropic magnetoresistance (Figure 5). Such behavior of galvanomagnetic properties proves the ferromagnetism of GaMnAs/GaAs structures produced by a combination of pulsed laser deposition in vacuum and laser annealing.

It is known that Hall resistance is described by expression

$$R_H = R_0\mu_0 H/d + R_A\mu_0 M/d, \quad (1)$$

where $d$ is the layer thickness, $\mu_0$ is the vacuum permeability, $H$ is the magnetic field strength, $M$ is the magnetization; $R_0$ is the normal Hall effect constant; $R_A$ is the anomalous Hall effect constant. The first term on the right-hand side of the equation describes the contribution of the normal Hall effect, the second term describes the contribution of the anomalous Hall effect (AHE). Figure 5, *a* shows that AHE prevails at temperatures below the Curie temperature and

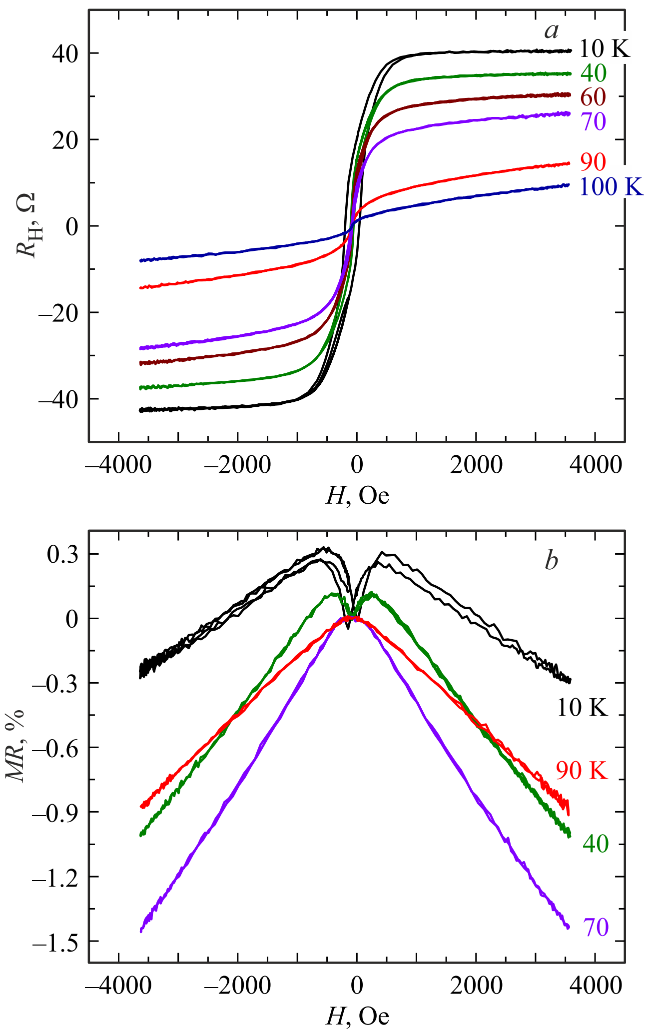


**Figure 5.** Magnetic field dependences of Hall resistance (*a*) and magnetoresistance (*b*) for the laser annealed B structure sample with GaMnAs layer produced by the PLD method at 250°C.

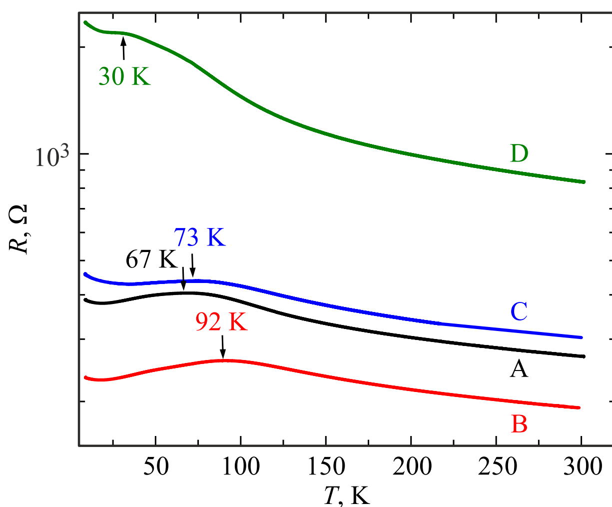


**Figure 4.** Temperature dependences of resistance of the annealed structures with GaMnAs layer produced at various temperatures. The structures are described in Table 1.

the Hall resistance in this case may be calculated as follows $R_H \sim R_A\mu_0 M/d$. This fact is used to determine spontaneous Hall resistance $R_H^S$ [17] which is proportional to spontaneous magnetization $M_S$ and characterizes ferromagnetic ordering in structures. Arrott's procedure [18] was used to plot dependence $M^2(H/M)$ and find $M_S$ by extrapolation of its linear portion up to the intersection with the vertical axis. $R_H^S$ was found in the same way, but using dependences $R_H^2(H/R_H)$.

If linear extrapolation $R_H^2(H/R_H)$ to $H = 0$ gives $(R_H^S)^2 > 0$, then ferromagnetic ordering is present for this measurement temperature. If $(R_H^S)^2 < 0$, the ferromagnetism is absent. Figure 6, *a* shows dependences $R_H^S(T)$ obtained by the method described above. The provided data also allow to find the ferromagnetic–paramagnetic phase transition temperature for each studied structure (detail in Figure 6, *a*). Comparing the obtained data with the Curie temperature assessment by the maximum position

on the corresponding temperature-resistance dependences (Figure 4), we can infer that the best match in determining $T_C$ by both methods is observed for structure B, as for A, C and D samples, assessment of $T_C$ by the maximum resistance position gives underestimated results. This observation is supported by the obtained dependences of coercive field vs. temperature (Figure 6, *b*). Thus, for structures A and D, hysteresis is recorded on the magnetic field dependences of Hall resistance at temperatures above 70 and 30 K, respectively, which indicates the presence of ferromagnetic properties in the GaMnAs layer.

Figure 7 shows the hole concentration at room temperature and the Curie temperature derived from temperature dependences of spontaneous Hall resistance for GaMnAs/GaAs structures produced by the PLD method at various temperatures and laser annealed.

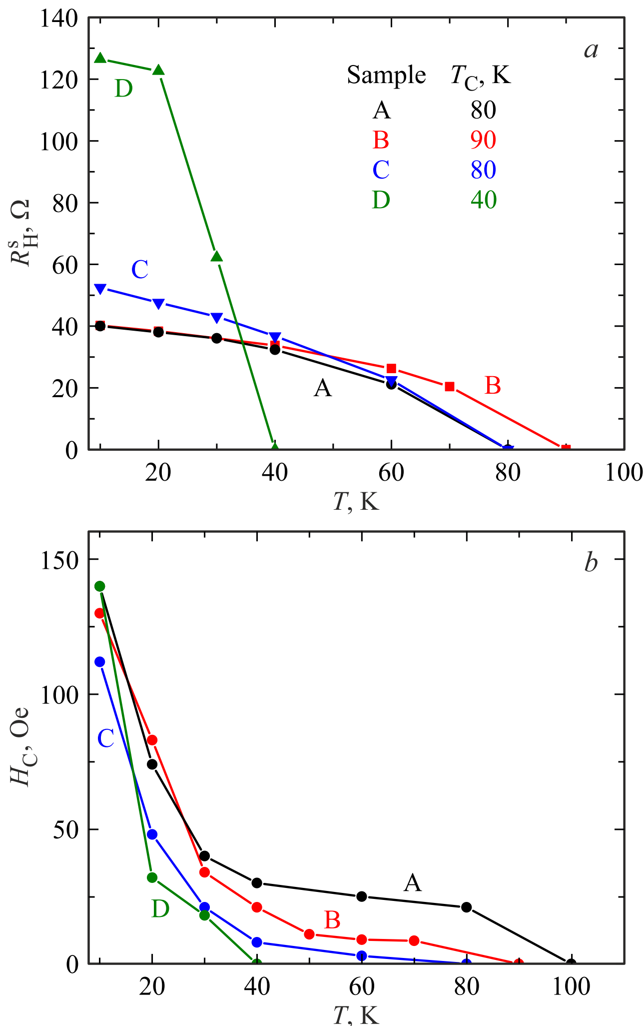


**Figure 6.** *a* — Temperature dependences of spontaneous Hall resistance proportional to the spontaneous magnetization which was determined using Arrott's procedure, and *b* — temperature dependences of coercive field of structures with GaMnAs layer produced at various temperatures by the pulsed laser deposition method and laser annealed (as described in Table 1).

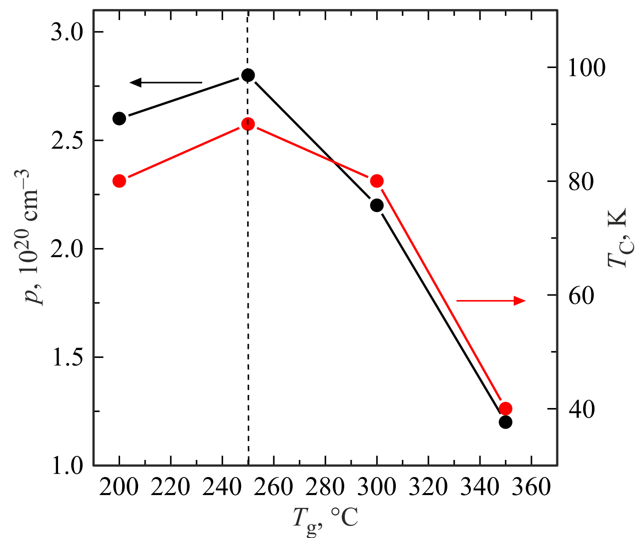


**Figure 7.** The hole concentration at room temperature and the Curie temperature derived from temperature dependences of spontaneous Hall resistance for GaMnAs/GaAs structures produced by the PLD method at various temperatures and laser annealed (Table 1).

Comparison of these two dependences suggests two conclusions: 1) hole concentration and ferromagnetic–paramagnetic phase transition temperature behavior depending on the structure growing temperature look similar; 2) some GaMnAs layer formation temperature (about 250°C) exists which is the best for achievement of the highest carrier concentrations and $T_C$ after laser exposure.

The first conclusion is in agreement with the literature data, because the Curie temperature in GaMnAs, taking into account the fact that it is proportional to $Mn_{Ga}$ concentration and concentration of electrically active holes ($p$) [19], is more often calculated as follows:

$$T_C \sim [\mathrm{Mn_{Ga}}] \cdot p^{1/3}, \tag{2}$$

where $p = [\mathrm{Mn_{Ga}}] - 2([\mathrm{As_{Ga}}] + [\mathrm{Mn}_i])$. Therefore, the maximum ferromagnetic–paramagnetic phase transition temperature is achieved at the maximum concentration of holes, $Mn_{Ga}$ acceptors and minimum concentrations of $n$-type point defects: antistructural arsenic defects in gallium position ($As_{Ga}$) and manganese in interstice ($Mn_i$).

The second conclusion concerns the ferromagnetic GaMnAs single-phase layer production technique addressed herein. The technique is based on the combination of the pulsed laser deposition and postgrowth pulsed laser annealing methods.

## 4. Conclusion

Thus, the study has shown that the use of pulsed laser annealing for postgrowth processing of GaMnAs layers

produced by pulsed laser deposition in vacuum at low temperatures of substrate (200–350°C) has a significant influence on their structural, electrophysical and magnetic properties. In particular, an intense coupled phonon-plasmon mode occurs in the Raman scattering spectra for annealed samples and considerable growth of hole conductivity in layers is observed (layer resistance becomes five orders lower). Magnetic properties of GaMnAs layers also vary considerably: the initial structures exhibited nonlinear magnetic field dependences of magnetization with hysteresis loop at room temperature of measurements which are attributed to the presence ferromagnetic semimetallic MnAs inclusions in the layers. After laser annealing, the dependences of magnetization on the external magnetic field become linear and the study of galvanomagnetic properties at low temperatures (from 10 to 150 K) shows that ferromagnetism exists in GaMnAs layers with the Curie temperature up to 90 K. The observed effects suggest that the used pulsed laser exposure results in modification (dissolution) of MnAs inclusions, electrical activation of Mn and, therefore, to formation of single-phase ferromagnetic GaMnAs semiconductor.

### Funding

The study was sponsored by the Russian Scientific Foundation (grant No. 23-29-00312).

### Conflict of interest

The authors declare that they have no conflict of interest.

## References

[1] M. Tanaka. Jpn. J. Appl. Phys. **60**, 010101 (2021).
[2] C. Song, B. Cui, F. Li, X. Zhou, F. Pan. Prog. Mater. Sci. **87**, 33 (2017).
[3] A. Hirohata, K. Yamada, Y. Nakatani, I.-L. Prejbeanu, B. Dieny, P. Pirro, B. Hillebrands. J. Magn. Magn. Mater. **509**, 166711 (2020).
[4] L.B. Chandrasekar, K. Gnanasekar, M. Karunakaran. Superlatt. Microstruct. **136**, 106322 (2019).
[5] S. Bhatti, R. Sbiaa, A. Hirohata, H. Ohno, S. Fukami, S.N. Piramanayagam. Mater. Today **20**, *9*, 530 (2017).
[6] M. Tanaka, S. Ohya, P.N. Hai. Appl. Phys. Rev. **1**, 011102 (2014).
[7] T. Dietl, H. Ohno, F. Matsukura, J. Cibert, D. Ferrand. Science **287**, 1019 (2000).
[8] K. Khazen, H.J. von Bardeleben, J.L. Cantin, A. Mauger, L. Chen, J.H. Zhao. Phys. Rev. B **81**, 235201 (2010).
[9] K. Takamura, F. Matsukura, Y. Ohno, H. Ohno. J. Appl. Phys. **81**, *8*, 4862 (1997).
[10] P.N. Hai, W. Nomura, T. Yatsui, M. Ohtsu, M. Tanaka. Appl. Phys. Lett. **101**, 193102 (2012).
[11] I.L. Kalentyeva, O.V. Vikhrova, Yu.A. Danilov, M.V. Dorokhin, B.N. Zvonkov, Yu.M. Kuznetsv, A.V. Kudrin, D.V. Khomitsky, A.E. Parafin, P.A. Yunin, D.V. Danilov. J. Magn. Magn. Mater. **556**, 169360 (2022).
[12] I.T. Yoon, T.W. Kang. J. Magn. Magn. Mater. **321**, 2257 (2009).
[13] W. Limmer, M. Glunk, S. Mascheck, A. Koeder, D. Klarer, W. Schoch, K. Thonke, R. Sauer, A. Waag. Phys. Rev. B **66**, 205209 (2002).
[14] K. Wan, J.F. Young. Phys. Rev. B **41**, 10772 (1990).
[15] O.V. Vikhrova, Yu.A. Danilov, B.N. Zvonkov, I.L. Kalent'eva, Yu.M. Kuznetsov, A.V. Nezhdanov, A.E. Parafin, D.V. Khomitsky, I.N. Antonov. FTT **63**, *3*, 346 (2021). (in Russian).
[16] J. Paitz. Krist. Techn. **7**, *9*, 999 (1972).
[17] H. Onho. J. Magn. Magn. Mater. **200**, 110 (1999).
[18] A. Arrott. Phys. Rev. **108**, 1394 (1957).
[19] Y.L. Soo, G. Kioseoglou, S. Kim, X. Chen, H. Luo, Y.H. Kao, Y. Sasaki, X. Liu, J.K. Furdyna. Appl. Phys. Lett. **80**, 2654 (2002).

*Translated by E.Ilyinskaya*